ISSN No:-2456-2165 https://doi.org/10.38124/ijisrt/26jan951

Dynamical Behavior and Optimal Control Analysis of a Stochastic Influenza Model with Quarantine

Md. Habibur Rahman[1]; Md. Abdullah Bin Masud[1,2]; Mostak Ahmed[1]; Tania Annur[2]; Sharmina Rahman[2]

[1]Department of Mathematics, Jagannath University, Dhaka, 1100, Bangladesh
[2]Department of CSE CSIT, Shanto-Mariam University of Creative Technology, Dhaka, 1230, Bangladesh

Publication Date: 2026/01/29

Abstract: This study investigates the transmission dynamics of influenza through an SEIQR framework incorporating both deterministic and stochastic effects. The model explicitly accounts for quarantine, vaccination, social distancing, and treatment as time-dependent control strategies. The analytical investigation involves computing the basic reproduction number and establishing both local and global stability properties of the disease-free and endemic equilibrium states through Lyapunov-based techniques. An optimal control problem is formulated to minimize the combined cost of infection prevalence, quarantine burden, and intervention efforts, and the necessary optimality conditions are obtained via Pontryagin's Maximum Principle. To capture environmental and behavioral uncertainties, stochastic perturbations driven by independent Wiener processes are introduced, and numerical solutions are obtained using the Euler–Maruyama scheme. Simulation results demonstrate that the implementation of optimal combined control strategies significantly suppresses infection levels and reduces stochastic fluctuations compared to uncontrolled scenarios. The findings highlight the effectiveness and robustness of integrated intervention policies for mitigating influenza outbreaks under uncertainty.

Keywords: *Influenza, Optimal Control, Pontryagin's Maximum Principle, Stochastic Model, Brownian Motion,*

How to Cite: Md. Habibur Rahman; Md. Abdullah Bin Masud; Mostak Ahmed; Tania Annur; Sharmina Rahman (2026) Dynamical Behavior and Optimal Control Analysis of a Stochastic Influenza Model with Quarantine. *International Journal of Innovative Science and Research Technology,* 11(1), 2202-2220. https://doi.org/10.38124/ijisrt/26jan951

I. INTRODUCTION

Influenza is a rapidly spreading acute respiratory infection that remains a persistent global public health concern, contributing significantly to morbidity and mortality each year. The disease is caused by influenza viruses of types A, B, and C, among which type A viruses are responsible for large-scale pandemics, type B viruses typically lead to regional epidemics, and type C viruses cause relatively mild infections with limited transmission [Abdoon and Alzahrani, 2024, Abdoon et~al., 2023, Alexander et~al., 2004]. Influenza is mainly transmitted via respiratory droplets expelled during coughing, sneezing, or close person-to-person interactions, with transmission risk increasing in densely populated settings [Almutairi et~al., 2023, Alsubaie et~al., 2024, Alzahrani et~al., 2023, Masud and Ahmed, 2018]. Following an incubation period of approximately one to four days, infected individuals may develop symptoms such as fever, headache, sore throat, nasal congestion, myalgia, and fatigue [Andreu-Vilarroig et~al., 2024, Arun~Kumar and Venkatesh, 2023, Ahmed et~al., 2023]. Although most cases are self-limiting, severe complications and fatalities are common among high-risk groups, including the elderly, young children, pregnant women, and individuals with underlying chronic conditions [Barik et~al., 2021, Masud et~al., 2021, Masud et~al., 2024].

Historically, influenza outbreaks have recurred across centuries, causing substantial demographic and socioeconomic disruption. The 1918 Spanish influenza pandemic remains the most catastrophic, infecting nearly one-third of the world's population and causing an estimated 50 million deaths worldwide [Kharis and Arifudin, 2017, Khondaker, 2022, Kim et~al., 2016, Lamwong et~al., 2022]. More recently, the 2009 A(H1N1) pandemic rapidly spread across more than 214 countries, resulting in over 18,000 confirmed deaths by August 2010 [Lamwong et~al., 2023, Lee et~al., 2010, Nainggolan, 2022]. Influenza outbreaks are broadly classified as seasonal, pandemic, zoonotic, or variant-related, with seasonal influenza posing a recurrent annual challenge that necessitates sustained preparedness and effective intervention strategies [Nainggolan, 2023, Ojo et~al., 2022, Parvin et~al., 2025, Masud et~al., 2017]. These recurring outbreaks highlight the importance of developing robust analytical tools to understand transmission dynamics and evaluate control measures.

ISSN No:-2456-2165 https://doi.org/10.38124/ijisrt/26jan951

Mathematical modeling has emerged as a powerful framework for studying influenza transmission and assessing the effectiveness of intervention strategies. Classical compartmental models such as the SIR and SEIR frameworks have been widely used to investigate disease dynamics and control mechanisms [Pongsumpun, 2017, Pongsumpun et~al., 2023, Prieto and Ibarguen-Mondragon, 2019, Masud et~al., 2026]. Several extensions of these models have incorporated additional epidemiological features, including treatment, vaccination, isolation, and temporary immunity, leading to formulations such as SIRC, SITR, SEITR, and SVEIHR models [Prosper et~al., 2011, Qiu and Feng, 2009, Rahmalia and Herlambang, 2018, Masud and Ahmed, 2025]. While these models provide valuable insights, many focus primarily on vaccination or treatment as isolated control strategies and often neglect the explicit role of quarantine as a core intervention.

Optimal control theory has been extensively applied to influenza models to identify time-dependent intervention strategies that minimize disease burden and implementation costs. Studies have demonstrated the effectiveness of vaccination, antiviral treatment, and reduced contact rates in suppressing outbreaks [Ratti et~al., 2023, Sabir et~al., 2022, Varshney and Dwivedi, 2021, Masud et~al., 2025]. For instance, Qiu and Feng showed that excessive reliance on antiviral treatment without adequate vaccination may paradoxically increase transmission [Waleed et~al., 2015, Ashraf et~al., 2025], while they emphasized the critical role of vaccine efficacy and coverage [World Health Organization, 2018]. The researcher further illustrated that combining pharmaceutical and non-pharmaceutical interventions leads to more effective disease mitigation [Rahman et~al., 2025, Imran et~al., 2019, Kanyiri et~al., 2020]. However, despite these advances, relatively few studies have simultaneously incorporated vaccination, treatment, and quarantine within a unified optimal control framework that also accounts for economic costs.

Quarantine is a crucial non-pharmaceutical intervention, particularly during periods of limited vaccine availability or emerging viral strains. Although isolation and quarantine measures have proven effective in controlling infectious diseases, their integration into influenza models remains limited. Some recent works have considered quarantine effects indirectly or as secondary measures [Varshney and Dwivedi, 2021, Lee et~al., 2010], but a comprehensive analysis that treats quarantine as a primary control variable alongside vaccination and treatment is still lacking. This gap motivates the need for a more realistic modeling framework that captures the combined impact of multiple interventions on influenza transmission dynamics.

In this study, we address this gap by proposing a novel Susceptible–Exposed –Infectious–Quarantined–Recovered (SEIQR) model for influenza transmission. The model explicitly incorporates quarantine as a key control mechanism and integrates multiple time-dependent control strategies within an optimal control framework. The qualitative behavior of the model is analyzed through equilibrium and stability theory, while Pontryagin's Maximum Principle is employed to characterize optimal intervention strategies. A cost-effectiveness analysis is further conducted to evaluate the trade-offs between disease reduction and control implementation costs. The results provide meaningful insights into the design of integrated, cost-effective strategies for influenza control and offer practical guidance for public health decision-makers.

II. MATERIALS AND METHODS

➢ *Mathematical Model*

To analyze the spread of influenza, we develop an SEIQR framework that partitions the population into five epidemiological classes. The model considers a closed population and captures the progression of individuals through different stages of infection and intervention. Seasonal effects are not introduced as explicit time-dependent forcing terms; instead, key parameters—most notably the transmission rate α—are assumed to represent the level of disease transmissibility during a given influenza season. This modeling choice reduces analytical complexity while retaining the core features of seasonal influenza transmission. Incorporating explicit seasonal variability in the transmission rate may be considered in future extensions of the model to account for time-varying epidemiological conditions. The state variables are defined as follows (see Fig. 1):

- $S(t)$: number of susceptible individuals,
- $E(t)$: number of exposed individuals,
- $I(t)$: number of infectious individuals,
- $Q(t)$: number of quarantined individuals,
- $R(t)$: number of recovered individuals.

Influenza transmission occurs mainly through respiratory droplets expelled when infected individuals cough, sneeze, or speak near others. Susceptible individuals may inhale these particles, resulting in subsequent infections. While transmission through contaminated surfaces (fomites) is possible, it plays a secondary role and is therefore not explicitly incorporated in the present framework. The infection process is governed by the transmission rate α, representing the probability of disease spread per contact under given environmental and behavioral conditions.

Once exposed, individuals experience an incubation period of average duration θ, during which they are infected but not infectious. They progress to the infectious class at rate $\kappa = 1/\theta$. Infectious individuals may then be quarantined at rate μ, while those in quarantine recover at rate δ_2. The natural death rate δ_1 applies uniformly across all compartments, and πN represents recruitment (or immigration) into the susceptible class. The complete model is expressed as:

ISSN No:-2456-2165 https://doi.org/10.38124/ijisrt/26jan951

$$\begin{cases} \frac{dS}{dt} = \pi N - \alpha SI - \delta_1 S, \\ \frac{dE}{dt} = \alpha SI - \left(\frac{1}{\theta} + \delta_1\right) E, \\ \frac{dI}{dt} = \frac{1}{\theta} E - (\mu + \delta_1) I, \\ \frac{dQ}{dt} = \mu I - (\delta_2 + \delta_1) Q, \\ \frac{dR}{dt} = \delta_2 Q - \delta_1 R, \end{cases} \quad (1)$$

Where the total population at time t satisfies

$$N = S(t) + E(t) + I(t) + Q(t) + R(t).$$

This SEIQR framework captures the essential mechanisms of influenza transmission and control, including exposure, quarantine, and recovery processes. The model parameters are summarized in Table 1. It is assumed that individuals who recover gain immunity that persists throughout the course of the epidemic. Over longer timescales, waning immunity may be represented by an SIRS-type extension, which could be explored in future studies. Assuming a constant total population, we have

$$\frac{dN}{dt} = 0 \quad \Rightarrow \quad \pi = \delta_1.$$

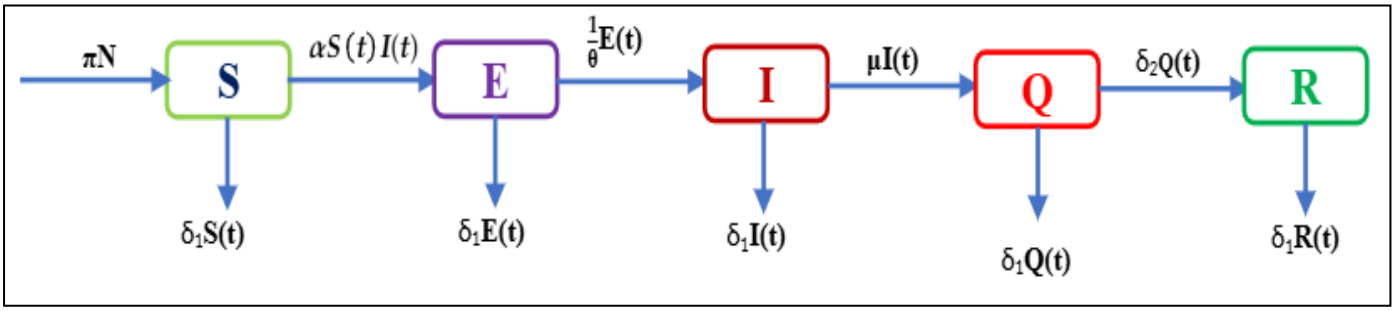

Fig 1 Flowchart of the SEIQR Influenza Transmission Model with Quarantine Intervention.

III. MODEL PARAMETERS

Table 1 Description of Model Parameters Used in the SEIQR Influenza Model. A Constant Total Population is Assumed with $\pi = \delta_1$.

Parameter	Definition	Value	Reference
N	Total human population	100	Assumed
π	Birth rate	$1/(365 \times 70)$	[Kanyiri et~al., 2018]
α	Infection rate of influenza virus	0.5	Assumed
δ_1	Natural death rate	$1/(365 \times 70)$	[Kanyiri et~al., 2018]
θ	Incubation period (days)	5	[Kanyiri et~al., 2018, Alexander et~al., 2004]
μ	Quarantine rate	$1/7$	[Kanyiri et~al., 2018, Alexander et~al., 2004]
δ_2	Recovery rate from quarantine	$1/14$	[Kanyiri et~al., 2018]
ν	Vaccination rate	0.2	Assumed
ϕ	Treatment efficacy	$1/14$	Assumed

➢ *Normalized Model*

To simplify the system, each compartment is normalized by the total population N:

$$s(t) = \frac{S(t)}{N}, \quad e(t) = \frac{E(t)}{N}, \quad i(t) = \frac{I(t)}{N}, \quad q(t) = \frac{Q(t)}{N}, \quad r(t) = \frac{R(t)}{N}.$$

The normalized SEIQR model becomes:

$$\begin{cases} \frac{ds}{dt} = \pi - \alpha si - \pi s, \\ \frac{de}{dt} = \alpha si - \left(\frac{1}{\theta} + \pi\right) e, \\ \frac{di}{dt} = \frac{1}{\theta} e - (\mu + \pi) i, \\ \frac{dq}{dt} = \mu i - (\delta_2 + \pi) q, \\ \frac{dr}{dt} = \delta_2 q - \pi r, \end{cases} \quad (2)$$

Where $r(t) = 1 - s(t) - e(t) - i(t) - q(t)$.

- Proposition 1. Let $(S(t), E(t), I(t), Q(t), R(t))$ denote the solutions of the SEIQR system in Eq. (1). The biologically feasible region is forward invariant; that is, if the initial conditions start in Γ, they remain in Γ for all $t \geq 0$.

$$\Gamma = \{(S, E, I, Q, R) \in \mathbb{R}_+^5 \quad | \quad 0 \leq S, E, I, Q, R \leq N\}$$

➢ *Equilibrium Points*

Setting the right-hand sides of Eq. (1) to zero gives:

- Disease-free equilibrium (DFE):

$$E_0 = (S^*, E^*, I^*, Q^*, R^*) = (N, 0, 0, 0, 0).$$

- Endemic equilibrium (EE), which exists only if $R_0 > 1$:

$$E_1 = (S^\dagger, E^\dagger, I^\dagger, Q^\dagger, R^\dagger),$$

ISSN No:-2456-2165 https://doi.org/10.38124/ijisrt/26jan951

With components

$$S^{\dagger} = \frac{N}{R_0},$$

$$I^{\dagger} = \frac{\pi N(R_0 - 1)}{R_0(1 + \pi\theta)(\mu + \pi)},$$

$$E^{\dagger} = \theta(\mu + \pi)I^{\dagger} = \frac{\pi N\theta(R_0 - 1)}{R_0(1 + \pi\theta)},$$

$$Q^{\dagger} = \frac{\mu I^{\dagger}}{\delta_2 + \pi},$$

$$R^{\dagger} = \frac{\delta_2 Q^{\dagger}}{\pi}.$$

- *Basic Reproduction Number*

Using the next-generation matrix method with infected compartments (E, I):

$$F = \begin{bmatrix} 0 & \alpha S \\ 0 & 0 \end{bmatrix}, \qquad V = \begin{bmatrix} \frac{1}{\theta} + \pi & 0 \\ -\frac{1}{\theta} & \mu + \pi \end{bmatrix}.$$

At the DFE ($S = N$):

$$F = \begin{bmatrix} 0 & \alpha N \\ 0 & 0 \end{bmatrix}.$$

Then

$$FV^{-1} = \begin{bmatrix} \frac{\alpha N}{(1 + \pi\theta)(\mu + \pi)} & \frac{\alpha N}{\mu + \pi} \\ 0 & 0 \end{bmatrix}.$$

The spectral radius of FV^{-1} gives the basic reproduction number:

$$R_0 = \frac{\alpha N}{(1+\pi\theta)(\pi+\mu)}. \tag{3}$$

- Existence Condition: The endemic equilibrium E_1 exists and is biologically meaningful if and only if $R_0 > 1$. For $R_0 \leq 1$, only the DFE exists.

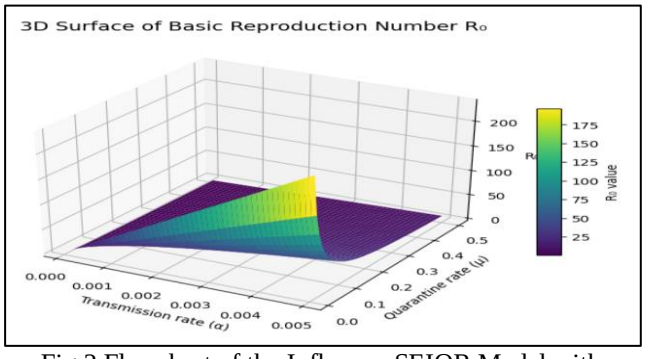

Fig 2 Flowchart of the Influenza SEIQR Model with Quarantine (Absolute Population).

Schematic Figure 2 representation of the SEIQR influenza transmission model in terms of absolute population sizes. The diagram illustrates the movement of individuals among the susceptible (S), exposed (E), infectious (I), quarantined (Q), and recovered (R) compartments. Susceptible individuals become exposed through effective contact with infectious individuals at rate α. Exposed individuals progress to the infectious class after the incubation period. Infectious individuals may be isolated through quarantine at rate μ, while quarantined individuals recover at rate δ_2. Natural birth and death processes are incorporated uniformly across all compartments.

- Theorem 1 *The disease–free equilibrium is locally asymptotically stable whenever* $R_0 < 1$.

- *Proof.* The local stability of the disease–free equilibrium E_0 is determined by the eigenvalues of the Jacobian matrix evaluated at E_0. These eigenvalues are obtained from the characteristic equation

$$\det(J_{E_0} - \lambda I) = 0.$$

Solving this equation yields the following eigenvalues:

$$\lambda_{1,2} = -\pi, \qquad \lambda_3 = -\pi - \delta_2,$$

$$\lambda_4 = \frac{1}{2\theta}\left[-1 - \theta(2b + \mu) - \sqrt{(\theta\mu - 1)^2 + 4\alpha\theta N}\right],$$

$$\lambda_5 = \frac{1}{2\theta}\left[-1 - \theta(2b + \mu) + \sqrt{(\theta\mu - 1)^2 + 4\alpha\theta N}\right].$$

It is clear that the eigenvalues λ_1, λ_2, λ_3, and λ_4 are strictly negative. Moreover, λ_5 is also negative provided that $R_0 < 1$. Hence, all eigenvalues of the Jacobian matrix have negative real parts under this condition. Consequently, the disease–free equilibrium E_0 is locally asymptotically stable for $R_0 < 1$.

- Theorem 2 *The endemic equilibrium is locally asymptotically stable whenever* $R_0 > 1$.

- *Proof.* To investigate the local stability of the endemic equilibrium E^*, we employ the Routh–Hurwitz stability criterion. The Jacobian matrix evaluated at E^* admits the eigenvalues together with three additional eigenvalues λ_3, λ_4, and λ_5 that satisfy the cubic characteristic equation

$$\lambda_1 = -\pi, \qquad \lambda_2 = -\pi - \delta_2,$$

$$\lambda^3 + a_2\lambda^2 + a_1\lambda + a_0 = 0.$$

The coefficients of this polynomial are given by

$$a_2 = \frac{1}{\theta} + \pi(2 + R_0),$$

ISSN No:-2456-2165 https://doi.org/10.38124/ijisrt/26jan951

$$a_1 = \frac{\pi(1 + 2\pi\theta + \theta\mu)R_0}{\theta},$$

$$a_0 = \frac{\pi(1 + \pi\theta)(\pi + \mu)(R_0 - 1)}{\theta}.$$

Since all model parameters are positive, it follows immediately that $a_2 > 0$ and $a_0 > 0$ whenever $R_0 > 1$. Moreover, direct computation yields

$$a_1 a_2 - a_0 = \frac{1}{\theta}(R_0 + \theta(R_0 + 1 + R_0)(1 + 2R_0))$$

$$+\mu(1 + R_0 + \theta R_0)$$

$$+\pi(1 + \theta\mu)(1 + R_0(3 + R_0)), \quad (4)$$

Which is strictly positive for $R_0 > 1$.

Therefore, all the Routh–Hurwitz conditions are satisfied. Consequently, the real parts of λ_3, λ_4, and λ_5 are negative. Combined with $\lambda_1 < 0$ and $\lambda_2 < 0$, this implies that the endemic equilibrium E^* is locally asymptotically stable for $R_0 > 1$.

➢ *Global Stability Analysis*

This section examines the global stability of the system in order to characterize its long-term dynamics for arbitrary initial states through rigorous mathematical analysis. A sufficient set of conditions ensuring global stability is established in the following theorem. Under these conditions, all solution trajectories of the system converge to the corresponding equilibrium point, independent of the initial configuration.

- Theorem 3 *Let* $E_0 = (s_1^*, e_1^*, i_1^*, q_1^*, r_1^*) = (1,0,0,0,0)$ *denote the disease–free equilibrium. Then* E_0 *is globally asymptotically stable in the feasible region* Γ *if and only if* $R_0 < 1$.

- *Proof.* To establish global stability, we construct the following Lyapunov function inspired by standard epidemic modeling techniques:

$$V(s, e, i, q) = (s - s_1^* \ln s) + e + i + q.$$

This function is nonnegative for all $(s, e, i, q) \in \Gamma$ and satisfies $V = 0$ at E_0.

Taking the derivative of V along the trajectories of the system yields

$$\frac{dV}{dt} = \left(1 - \frac{s_1^*}{s}\right)\frac{ds}{dt} + \frac{de}{dt} + \frac{di}{dt} + \frac{dq}{dt}.$$

Substituting the model equations gives

$$\frac{dV}{dt} = \left(1 - \frac{s_1^*}{s}\right)(\pi - (\pi + \alpha i N)s) + \left(\alpha i N s - \frac{1}{\theta}e\right)$$

$$+\left(\frac{1}{\theta}e - (\mu + \pi)i\right) + (\mu i - (\pi + \delta_2)q). \quad (5)$$

After simplification, this expression becomes

$$\frac{dV}{dt} = \pi\left(1 - \frac{s_1^*}{s}\right) - \pi s + \pi s_1^* + \alpha i N s_1^* - \pi e - \pi i - (\pi + \delta_2)q.$$

At the disease–free equilibrium, $s_1^* = 1$, which leads to

$$\frac{dV}{dt} = \pi\left[\left(1 - \frac{1}{s}\right) + (1 - s)\right] - \pi e - \pi i - (\pi + \delta_2)q.$$

This can be rewritten as

$$\frac{dV}{dt} = -\pi\left(\frac{s - 1}{s}\right)^2 - \pi e - \pi i - (\pi + \delta_2)q \le 0,$$

With equality holding if and only if $s = 1$, $e = 0$, $i = 0$, and $q = 0$.

Thus, $\frac{dV}{dt}$ is negative semidefinite in Γ, and the largest invariant set contained in $\left\{\frac{dV}{dt} = 0\right\}$ consists solely of the equilibrium point E_0. By LaSalle's invariance principle, the disease–free equilibrium E_0 is globally asymptotically stable on Γ whenever $R_0 < 1$.

- Theorem 4 *Assume that* $R_0 > 1$. *Let* $E^* = (s_2^*, e_2^*, i_2^*, q_2^*, r_2^*)$ *denote the endemic equilibrium given by Eq. (6). Then the equilibrium* E^* *of system Eq. (3) is globally asymptotically stable in the invariant region* Γ.

- *Proof.* To prove global stability, we introduce a Volterra–type Lyapunov function defined by

$$V(s, e, i, q, r) = \left(s - s_2^* - s_2^* \ln\frac{s}{s_2^*}\right) + \left(e - e_2^* - e_2^* \ln\frac{e}{e_2^*}\right)$$

$$+\left(i - i_2^* - i_2^* \ln\frac{i}{i_2^*}\right) + \left(q - q_2^* - q_2^* \ln\frac{q}{q_2^*}\right)$$

$$+\left(r - r_2^* - r_2^* \ln\frac{r}{r_2^*}\right). \quad (6)$$

This function is nonnegative for all $(s, e, i, q, r) \in \Gamma$ and satisfies $V = 0$ at the endemic equilibrium E^*.

Differentiating V with respect to time along the trajectories of the system yields

$$\frac{dV}{dt} = \left(1 - \frac{s_2^*}{s}\right)\frac{ds}{dt} + \left(1 - \frac{e_2^*}{e}\right)\frac{de}{dt}$$

$$+\left(1 - \frac{i_2^*}{i}\right)\frac{di}{dt} + \left(1 - \frac{q_2^*}{q}\right)\frac{dq}{dt} + \left(1 - \frac{r_2^*}{r}\right)\frac{dr}{dt}. \quad (7)$$

Substituting the right-hand sides of system *Eq. (1)* into the above expression gives

ISSN No:-2456-2165 https://doi.org/10.38124/ijisrt/26jan951

$$\frac{dV}{dt} = \left(1 - \frac{s_2^*}{s}\right)[\pi - (\pi + \alpha i N)s]$$

$$+\left(1 - \frac{e_2^*}{e}\right)\left[\alpha i N s - \left(\frac{1}{\theta} + \pi\right)e\right]$$

$$+\left(1 - \frac{i_2^*}{i}\right)\left[\frac{1}{\theta}e - (\mu + \pi)i\right]$$

$$+\left(1 - \frac{q_2^*}{q}\right)[\mu i - (\pi + \delta_2)q]$$

$$+\left(1 - \frac{r_2^*}{r}\right)[\delta_2 q - \pi r]. \quad (8)$$

Using the equilibrium relations satisfied by E^* and simplifying, it follows that

$$\frac{dV}{dt} \leq 0 \qquad \text{forall}(s, e, i, q, r) \in \Gamma,$$

With equality if and only if $(s, e, i, q, r) = (s_2^*, e_2^*, i_2^*, q_2^*, r_2^*)$.

Therefore, the derivative of V is negative semidefinite and the largest invariant set contained in $\left\{\frac{dV}{dt} = 0\right\}$ reduces to the endemic equilibrium E^*. By LaSalle's invariance principle, E^* is globally asymptotically stable in Γ whenever $R_0 > 1$.

Replace s with $s - s_2^*$, e with $e - e_2^*$, i with $i - i_2^*$, q with $q - q_2^*$, and r with $r - r_2^*$, then we have:

$$\frac{d\phi}{dt} = (1 - s_2^*)\{\ b - (\pi + \alpha i N)(s - s_2^*)\}$$

$$+\left(1 - \frac{e_2^*}{e}\right)\{\ \alpha i N s - \left(\frac{1}{\theta} + \pi\right)(e - e_2^*)\}$$

$$+\left(1 - \frac{i_2^*}{i}\right)\{\ \frac{1}{\theta}e - (\mu + \pi)(i - i_2^*)\}$$

$$+\left(1 - \frac{q_2^*}{q}\right)\{\ \mu i - (\pi + \delta_2)(q - q_2^*)\}$$

$$+\left(1 - \frac{r_2^*}{r}\right)\{\ \delta_2 q - \pi(r - r_2^*)\}. \quad (9)$$

$$\frac{d\phi}{dt} = b - \pi\left(\frac{s_2^*}{s}\right) - (\pi + \alpha i N)\frac{(s - s_2^*)^2}{s}$$

$$+\alpha i N s - \alpha i N s\left(\frac{e_2^*}{e}\right) - \left(\frac{1}{\theta}e\right)\frac{(e - e_2^*)^2}{e}$$

$$+\frac{1}{\theta}e - \frac{1}{\theta}e\left(\frac{i_2^*}{i}\right) - (\mu + \pi)\frac{(i - i_2^*)^2}{i}$$

$$+\mu i - \mu i\left(\frac{q_2^*}{q}\right) - (\pi + \delta_2)\frac{(q - q_2^*)^2}{q}$$

$$+\delta_2 q - \delta_2 q\left(\frac{r_2^*}{r}\right) - (r - r_2^*)^2 r. \quad (10)$$

Now, we have

$$\frac{d\phi}{dt} = K_1 - K_2,$$

Where

$$K_1 = b + \alpha i N s + \frac{1}{\theta}e + \mu i + \delta_2 q,$$

$$K_2 = \pi\left(\frac{s_2^*}{s}\right) + (\pi + \alpha i N)\frac{(s - s_2^*)^2}{s} + \alpha i N s\left(\frac{e_2^*}{e}\right)$$

$$+\left(\frac{1}{\theta} + \pi\right)\frac{(e - e_2^*)^2}{e} + \frac{1}{\theta}e\left(\frac{i_2^*}{i}\right)$$

$$+(\mu + \pi)\frac{(i - i_2^*)^2}{i} + \mu i\left(\frac{q_2^*}{q}\right) + (\pi + \delta_2)\frac{(q - q_2^*)^2}{q}$$

$$+\delta_2 q\left(\frac{r_2^*}{r}\right) + (r - r_2^*)^2 r. \quad (11)$$

It is evident that $\frac{d\phi}{dt} = 0$ when $K_1 < K_2$, and it equals zero when $s = s_2^*, e = e_2^*, i = i_2^*, q = q_2^*, r = r_2^*$ which aligns with the established principles. Therefore, the endemic equilibrium is globally asymptotically stable on Γ whenever $K_1 < K_2$.

➢ *Sensitivity Analysis*

Sensitivity analysis plays an essential role in assessing and improving the predictive capability of influenza transmission models. By evaluating how variations in model parameters affect system dynamics, this analysis helps to identify the most influential factors governing disease spread. A widely adopted technique is the normalized forward sensitivity index, which measures the proportional variation in an output variable induced by a relative change in a specific parameter. This method facilitates a systematic assessment and comparison of how individual parameters affect the model's behavior.

Such analysis is particularly important as it highlights parameters that exert the greatest control over disease transmission and progression. Identifying these key parameters supports the development of more efficient intervention strategies by directing resources toward the most impactful control measures. As a result, public health policies such as vaccination programs, social distancing measures, and treatment strategies can be better optimized to reduce disease burden and mitigate outbreaks.

The normalized forward sensitivity index is defined as

$$\Upsilon_{\vartheta}^{R_0} = \frac{\partial R_0}{\partial \vartheta} \cdot \frac{\vartheta}{R_0}.$$

ISSN No:-2456-2165 https://doi.org/10.38124/ijisrt/26jan951

Table 3 summarizes the sensitivity indices of the parameters included in the influenza model. Each index reflects the degree to which a parameter influences the basic reproduction number R_0, a fundamental indicator of disease transmissibility. A positive sensitivity index implies that increasing the parameter leads to an increase in R_0, whereas a negative value indicates a reduction in R_0. Notably, the results show that the total population size (N) and the birth rate (b) both have sensitivity indices equal to one, indicating that a 10% increase in either parameter produces a proportional 10% increase in R_0. This indicates that these parameters are directly and proportionally related to the potential spread of the disease. The sensitivity results indicate that the basic reproduction number R_0 is most sensitive to changes in the total population size N and the recruitment rate b, both exhibiting unit sensitivity indices. This implies a proportional relationship between these parameters and R_0. In contrast, the quarantine rate μ has a strong negative sensitivity index, suggesting that increasing quarantine effectiveness significantly reduces disease transmission. The remaining parameters show comparatively smaller effects, indicating lower influence on the epidemic threshold.

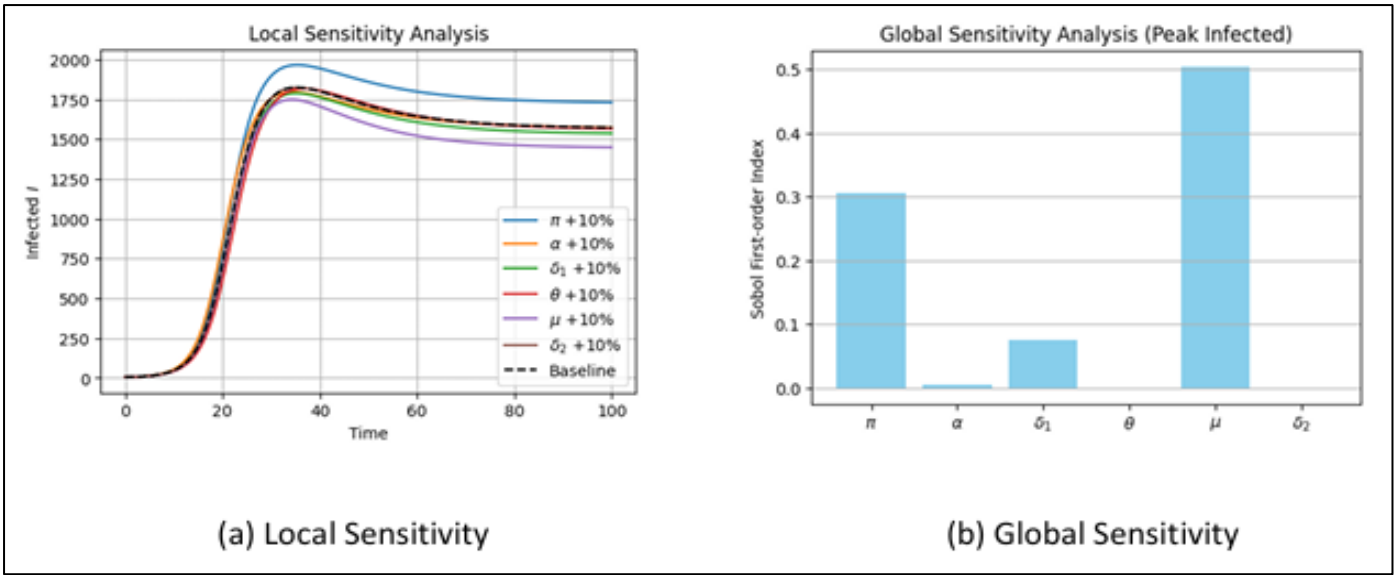

Fig 3 Scenario of Local and Global Sensitivity.

Table 2 Normalized Forward Sensitivity Indices of the Basic Reproduction Number R_0 with Respect to Key Model Parameters.

Parameter	Description	Sensitivity Index
N	Total human population	+1.00000
b	Recruitment (birth) rate	+1.00000
α	Influenza transmission rate	0.00046
θ	Incubation period	0.00019
μ	Quarantine rate	0.99972

IV. MATHEMATICAL MODEL WITH CONTROL VARIABLES

The optimal control problem provides a mathematical framework for determining time–dependent intervention strategies that steer a dynamical system toward a desired objective. In the present study, this framework is employed to analyze and regulate the transmission dynamics of influenza. The main goal is to mitigate the public health impact of the disease by appropriately influencing key epidemiological processes over a finite time horizon.

➢ *To this End, Four Control Functions are Introduced:*

- $u_1(t)$ denotes the vaccination control, representing the intensity of vaccine administration to susceptible individuals;
- $u_2(t)$ represents social intervention measures aimed at reducing effective contact rates;
- $u_3(t)$ corresponds to the treatment of infected individuals, which reduces both disease severity and infectiousness;
- $u_4(t)$ accounts for treatment and management of quarantined individuals, ensuring effective isolation and recovery.

These control variables are integrated into the influenza transmission model to influence the dynamics of the susceptible, exposed, infected, quarantined, and recovered compartments. The goal is to identify optimal control strategies that minimize the overall cost associated with both disease burden and the implementation of interventions.

ISSN No:-2456-2165 https://doi.org/10.38124/ijisrt/26jan951

The controlled influenza model is given by

$$\begin{cases} \frac{dS(t)}{dt} = \pi - \frac{(1-u_2(t))\alpha S(t)I(t)}{N} - \pi S(t) - \nu u_1(t), \\ \frac{dE(t)}{dt} = \frac{(1-u_2(t))\alpha S(t)I(t)}{N} - \left(\frac{1}{\theta} + \pi\right) E(t), \\ \frac{dI(t)}{dt} = \frac{1}{\theta} E(t) - (\mu + \pi) I(t) - \phi u_3(t) I(t), \\ \frac{dQ(t)}{dt} = \mu I(t) - (\pi + (1 + u_4(t))\delta_2) Q(t), \\ \frac{dR(t)}{dt} = (1 + u_4(t))\delta_2 Q(t) + \phi u_3(t) I(t) + \nu u_1(t) - \pi R(t). \end{cases} \quad (12)$$

From a mathematical perspective, the optimal control problem consists of the above system of state equations coupled with an objective functional that balances epidemiological outcomes against the costs associated with implementing control measures. The optimal control functions $u_1(t)$, $u_2(t)$, $u_3(t)$, and $u_4(t)$ are sought subject to admissible bounds and the governing dynamics.

To derive the necessary conditions for optimality, Pontryagin's Maximum Principle is applied. This principle converts the original control problem into an equivalent Hamiltonian system composed of state and adjoint equations, along with characterization conditions for the optimal controls. Analysis of this system guarantees the existence of optimal intervention strategies that achieve an effective balance between minimizing disease transmission and limiting the cost of control implementation.

$$J(u_1(t), u_2(t), u_3(t), u\_4(t)) = \int_0^T [\, C_1 I(t) + C_2 Q(t) + 12(W_1 u_1^2(t) + W_2 u_2^2(t) + W_3 u_3^2(t) + W_4 u_4^2(t))] \, dt,$$

Where B_i are positive weights for $i = 1,2, \ldots 6$.

We aim to determine the optimal control strategies $u_1^*(t), u_2^*(t), u_3^*(t)$, and $u_4^*(t)$ by formulating the corresponding Lagrangian functional of the optimal control problem, given by

$$\mathcal{L} = C_1 I(t) + C_2 Q(t) + \frac{1}{2}(W_1 u_1^2(t) + W_2 u_2^2(t) + W_3 u_3^2(t) + W_4 u_4^2(t)). \quad (13)$$

The solution of this optimal control problem provides the most effective combination of vaccination policies, non-pharmaceutical interventions, and treatment strategies necessary to reduce and control the spread of influenza within the population.

- Theorem 5 *For the optimal control problem under consideration, there exist adjoint variables* $\lambda_i(t)$, $i = 1,2,3,4,5$, *satisfying the adjoint system*

$$\frac{d\lambda_i}{dt} = -\frac{\partial H}{\partial \phi_i}, \quad (14)$$

Where $\phi = (S, E, I, Q, R)$ denotes the state vector. The transversality conditions are given by

$$\lambda_i(T) = 0, \qquad i = 1,2,3,4,5.$$

Moreover, the optimal control functions u_1^*, u_2^*, u_3^*, and u_4^* are characterized by

$$\begin{cases} u_1^* = \max\left\{0, \min\left\{1, \frac{(\lambda_1 - \lambda_5)\nu S(t)}{W_1}\right\}\right\}, \\ u_2^* = \max\left\{0, \min\left\{1, \frac{(\lambda_2 - \lambda_1)\alpha S(t)I(t)}{NW_2}\right\}\right\}, \\ u_3^* = \max\left\{0, \min\left\{1, \frac{(\lambda_3 - \lambda_5)\phi I(t)}{W_3}\right\}\right\}, \\ u_4^* = \max\left\{0, \min\left\{1, \frac{(\lambda_4 - \lambda_5)\delta_2 Q(t)}{W_4}\right\}\right\}. \end{cases} \quad (15)$$

- *Proof.* According to Pontryagin's Maximum Principle, the Hamiltonian function associated with the influenza control model is defined as

$$H = L(I(t), Q(t), u_1(t), u_2(t), u_3(t), u_4(t)) + \lambda_1 \dot{S}(t) + \lambda_2 \dot{E}(t) + \lambda_3 \dot{I}(t) + \lambda_4 \dot{Q}(t) + \lambda_5 \dot{R}(t), \quad (13)$$

Where $L(\cdot)$ denotes the running cost functional.

Substituting the state equations into the Hamiltonian yields

$$\begin{aligned} H = {} & C_1 I(t) + C_2 Q(t) + \frac{1}{2}(W_1 u_1^2(t) + W_2 u_2^2(t) + W_3 u_3^2(t) + W_4 u_4^2(t)) \\ & + \lambda_1(\pi - (1 - u_2(t))\frac{\alpha S(t)I(t)}{N} - \pi S(t) - \nu u_1(t) S(t)) \\ & + \lambda_2((1 - u_2(t))\frac{\alpha S(t)I(t)}{N} - \left(\frac{1}{\theta} + \pi\right) E(t)) \\ & + \lambda_3(\frac{1}{\theta} E(t) - (\mu + b) I(t) - a u_3(t) I(t)) \\ & + \lambda_4(\mu I(t) - (\pi + (1 + u_4(t))\delta_2) Q(t)) \\ & + \lambda_5((1 + u_4(t))\delta_2 Q(t) + a u_3(t) I(t) + \nu u_1(t) S(t) - \pi R(t)). \end{aligned} \quad (14)$$

The adjoint equations are obtained by differentiating the Hamiltonian with respect to the state variables:

$$\begin{aligned} \dot{\lambda}_1 &= -\frac{\partial H}{\partial S} = \lambda_1\left((1 - u_2^*)\frac{\alpha I}{N} + \pi + \nu u_1^*\right) - \lambda_2(1 - u_2^*)\frac{\alpha I}{N} - \lambda_5 \nu u_1^*, \\ \dot{\lambda}_2 &= -\frac{\partial H}{\partial E} = \left(\frac{1}{\theta} + \pi\right)\lambda_2 - \frac{1}{\theta}\lambda_3, \\ \dot{\lambda}_3 &= -\frac{\partial H}{\partial I} = (\lambda_1 - \lambda_2)(1 - u_2^*)\frac{\alpha S}{N} + \lambda_3(\mu + b + a u_3^*) - \mu\lambda_4 - a u_3^* \lambda_5 - C_1, \\ \dot{\lambda}_4 &= -\frac{\partial H}{\partial Q} = \lambda_4((1 + u_4^*)\delta_2 + \pi) - \lambda_5(1 + u_4^*)\delta_2 - C_2, \\ \dot{\lambda}_5 &= -\frac{\partial H}{\partial R} = \pi\lambda_5. \end{aligned} \quad (15)$$

Applying the optimality conditions $\frac{\partial H}{\partial u_j} = 0$, for $j = 1,2,3,4$, together with the control bounds $0 \le u_j \le 1$, leads to the explicit characterizations of the optimal controls given in equation (15). This completes the proof.

ISSN No:-2456-2165 https://doi.org/10.38124/ijisrt/26jan951

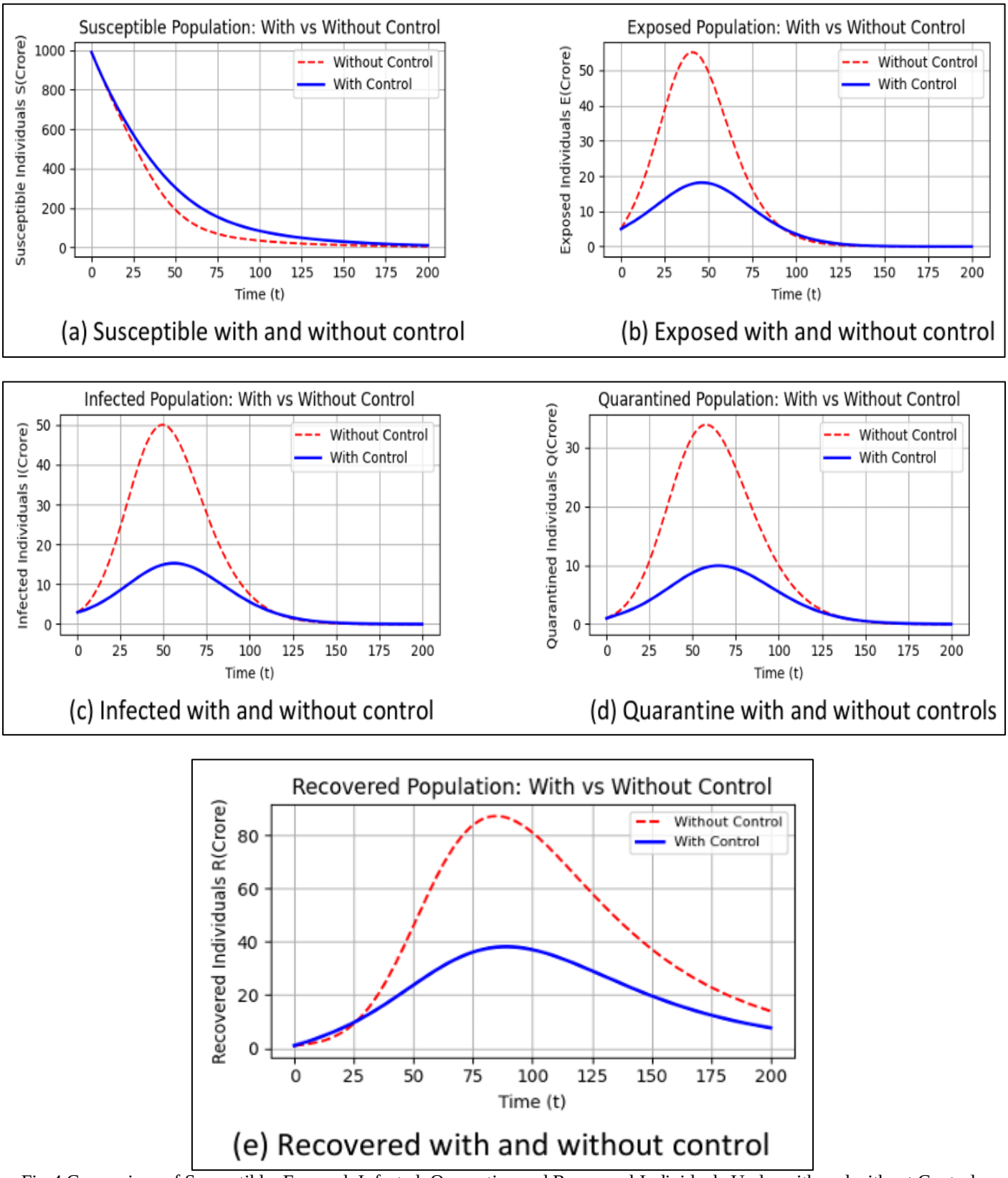

Fig 4 Comparison of Susceptible, Exposed, Infected, Quarantine and Recovered Individuals Under with and without Control.

ISSN No:-2456-2165 https://doi.org/10.38124/ijisrt/26jan951

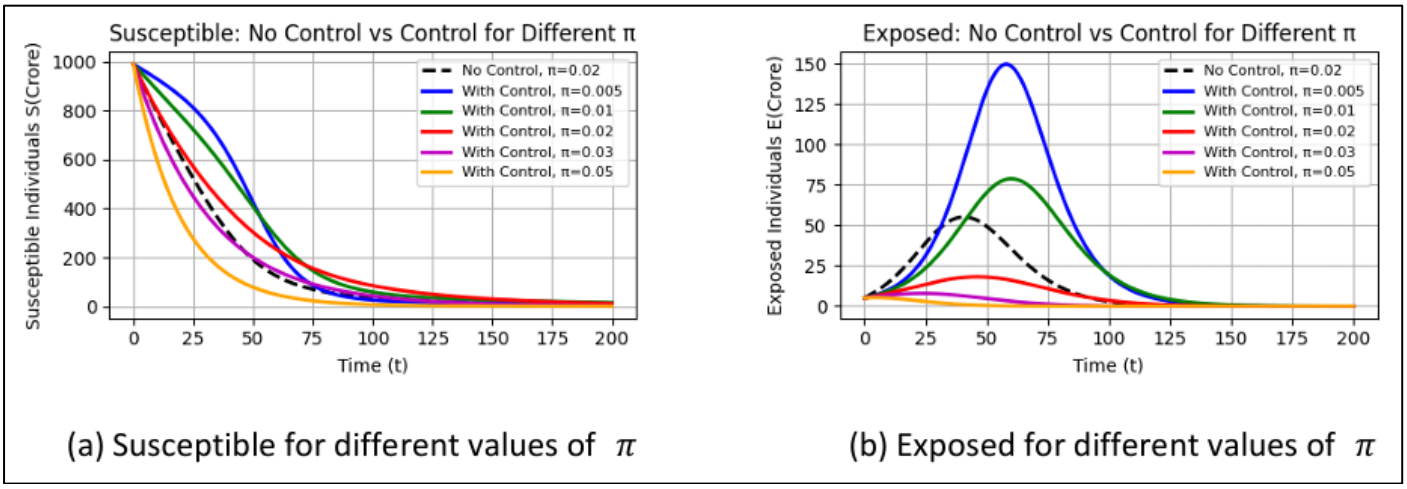

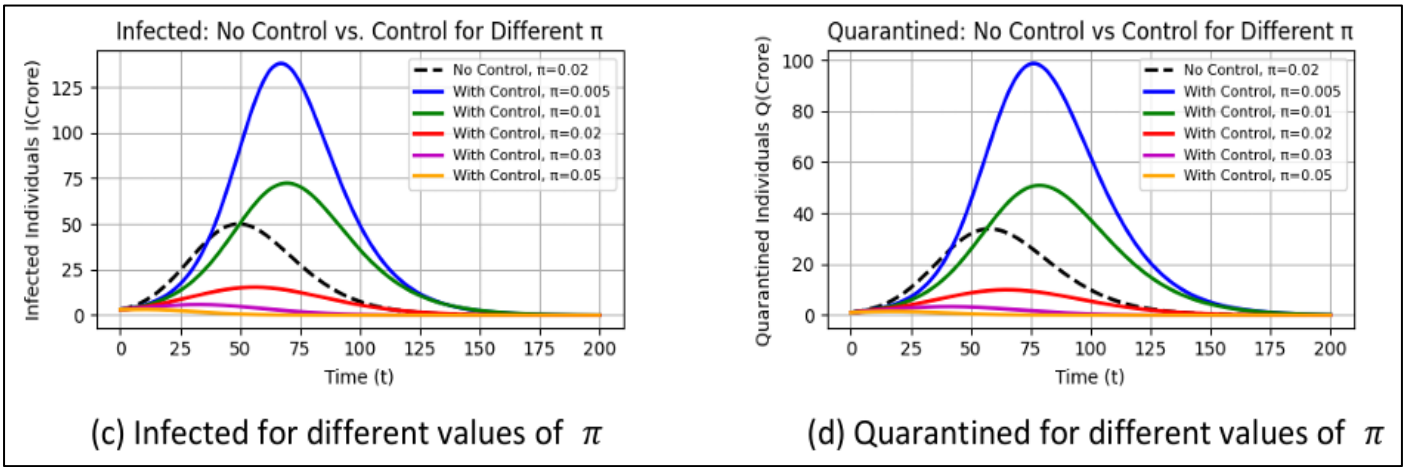

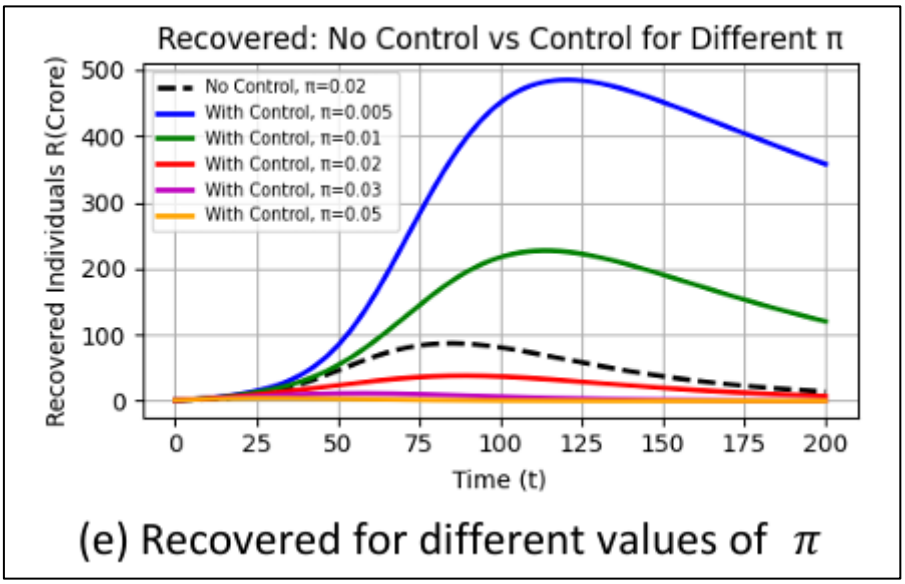

Fig 5 Comparison of Infected Individuals Under Various Control Scenarios, Including Isolation (u_1), Social Awareness (u_2), and Treatment (u_3), as well as without Control.

ISSN No:-2456-2165 https://doi.org/10.38124/ijisrt/26jan951

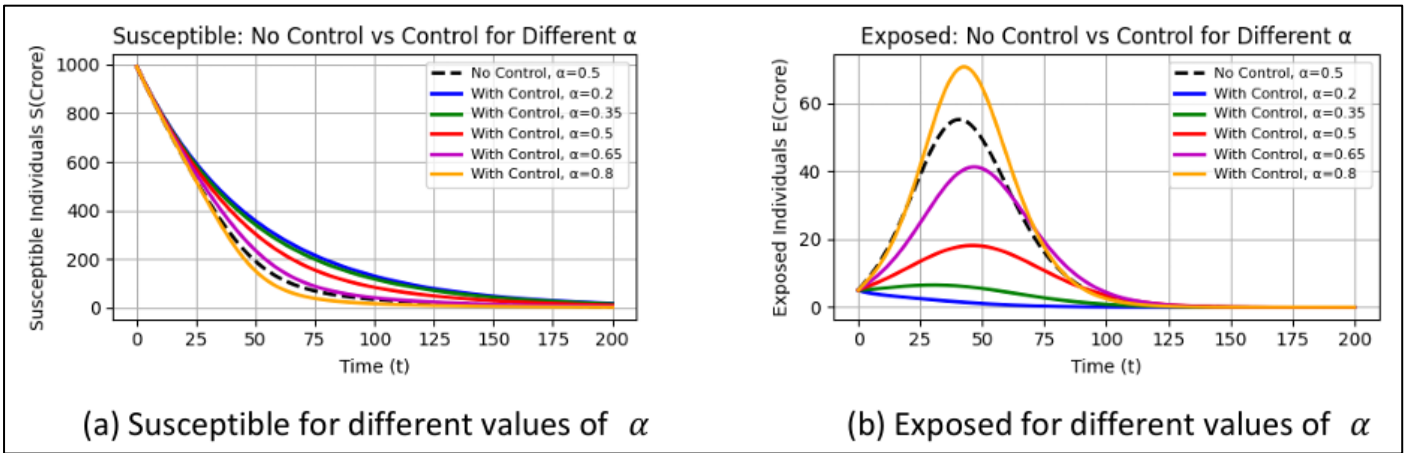

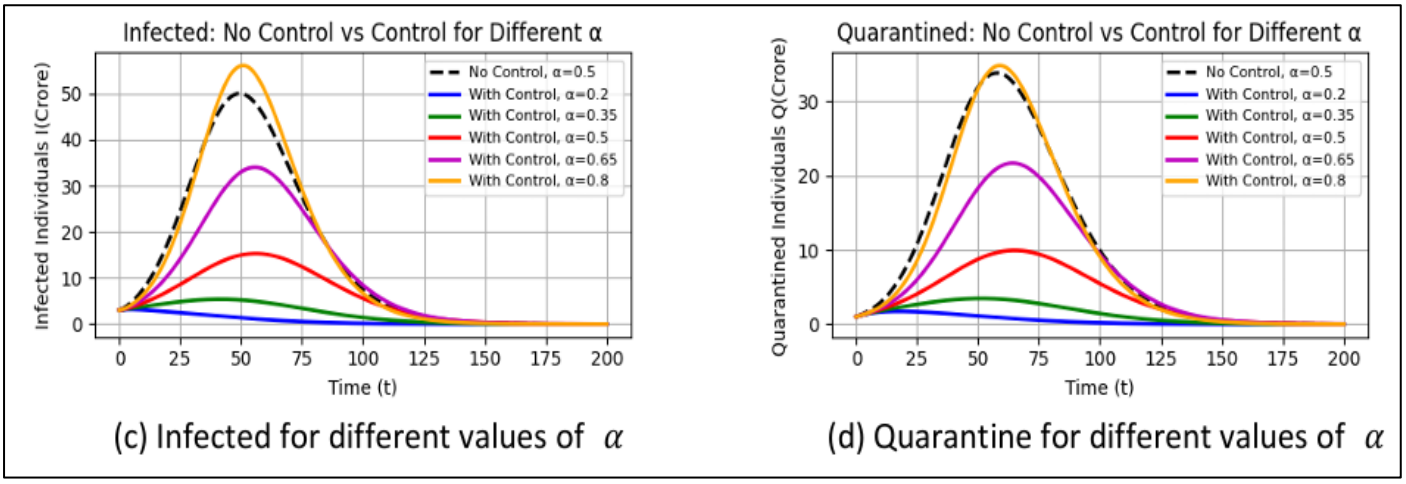

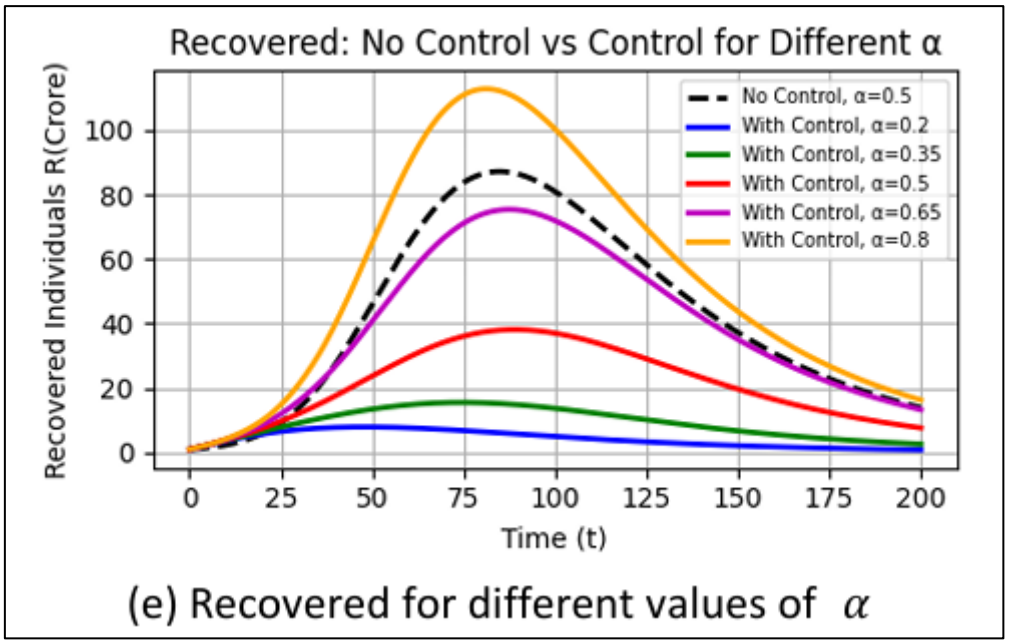

Fig 6 Comparison of Infected Individuals Under Various Control Scenarios, Including Isolation (u_1), Social Awareness (u_2), and Treatment (u_3), as well as without Control.

ISSN No:-2456-2165 https://doi.org/10.38124/ijisrt/26jan951

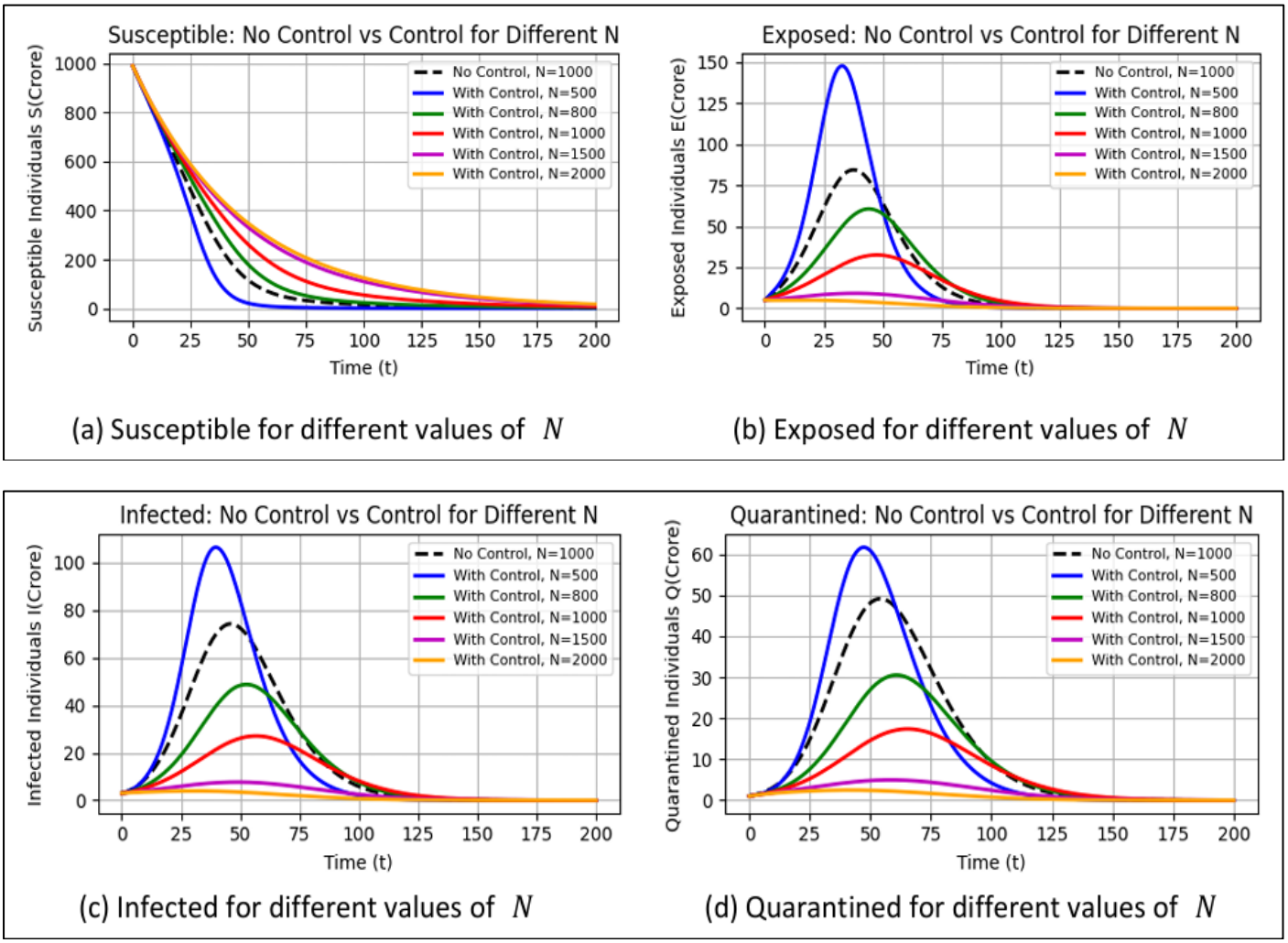

Fig 7 Comparison of Infected Individuals Under Various Control Scenarios, Including Isolation (u_1), Social Awareness (u_2), and Treatment (u_3), as well as without Control.

ISSN No:-2456-2165 https://doi.org/10.38124/ijisrt/26jan951

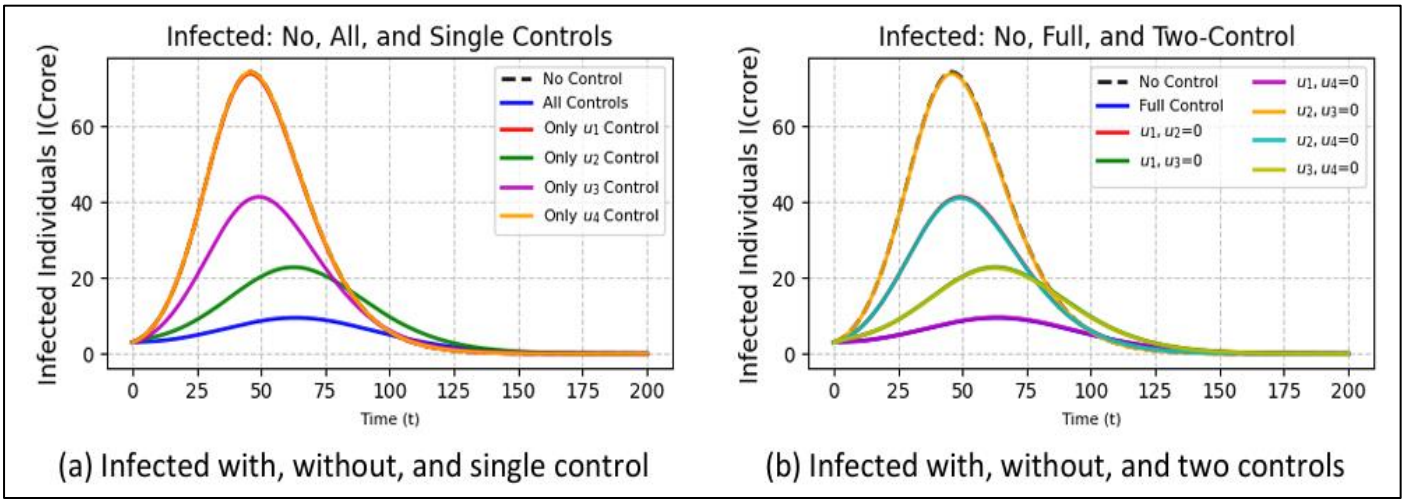

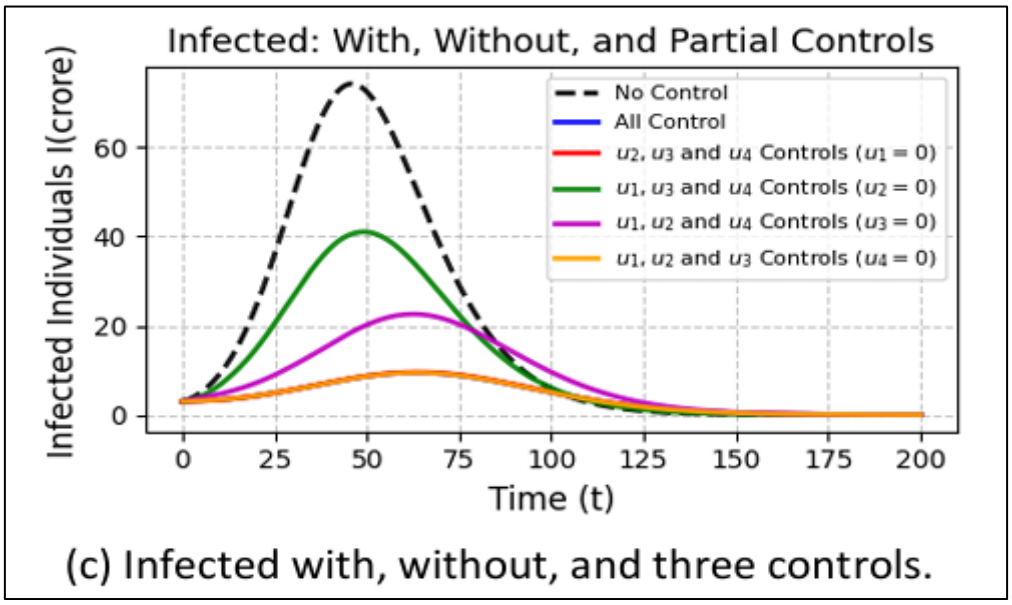

Fig 8 Comparison of Infected Individuals Under Various Control Scenarios, Including Isolation (u_1), Social Awareness (u_2), and Treatment (u_3), as well as without Control.

V. STOCHASTIC MODEL WITH CONTROL

We assume that random environmental fluctuations, behavioral uncertainty, and demographic variability affect the disease transmission and progression rates. These uncertainties are modeled by independent standard Wiener processes. Here, $W_i(t)$, $i = 1, \ldots, 5$, are independent standard Wiener processes defined on a complete probability space $(\Omega, \mathcal{F}, \mathbb{P})$. The parameters $\sigma_i > 0$ represent the intensity of stochastic perturbations affecting each epidemiological compartment. The stochastic terms capture random fluctuations arising from environmental variability, heterogeneity in contact patterns, and uncertainties in intervention effectiveness. When $\sigma_i = 0$, the stochastic model reduces to the deterministic system.

$$\begin{cases} dS(t) = [\pi - (1-u_2(t))\alpha\frac{S(t)I(t)}{N} - \pi S(t) - vu_1(t)]dt + \sigma_1 S(t)\ \ dW_1(t), \\ dE(t) = [(1-u_2(t))\alpha\frac{S(t)I(t)}{N} - \left(\frac{1}{\theta}+\pi\right)E(t)]dt + \sigma_2 E(t)\ \ dW_2(t), \\ dI(t) = [\frac{1}{\theta}E(t) - (\mu+\pi)I(t) - \phi u_3(t)I(t)]dt + \sigma_3 I(t)\ \ dW_3(t), \\ dQ(t) = [\mu I(t) - (\pi + (1+u_4(t))\delta_2)Q(t)]dt + \sigma_4 Q(t)\ \ dW_4(t), \\ dR(t) = [(1+u_4(t))\delta_2 Q(t) + \phi u_3(t)I(t) + vu_1(t) - \pi R(t)]dt + \sigma_5 R(t)\ \ dW_5(t). \end{cases} \quad (16)$$

The Hamiltonian for an optimal control problem is

$$\mathcal{H} = C_1 I(t) + C_2 Q(t) + \frac{1}{2}(W_1 u_1^2(t) + W_2 u_2^2(t) + W_3 u_3^2(t) + W_4 u_4^2(t)) \quad (17)$$

ISSN No:-2456-2165 https://doi.org/10.38124/ijisrt/26jan951

$$+\lambda_S \dot{S} + \lambda_E \dot{E} + \lambda_I \dot{I} + \lambda_Q \dot{Q} + \cdots \quad (18)$$

The co-state (adjoint) equations are obtained as

$$\dot{\lambda}_S = -\frac{\partial \mathcal{H}}{\partial S}, \lambda_S(T) = 0$$

$$\dot{\lambda}_E = -\frac{\partial \mathcal{H}}{\partial E}, \lambda_E(T) = 0$$

$$\dot{\lambda}_I = -\frac{\partial \mathcal{H}}{\partial I}, \lambda_I(T) = 0$$

$$\dot{\lambda}_Q = -\frac{\partial \mathcal{H}}{\partial Q}, \lambda_Q(T) = 0$$

The optimal controls are found by

$$\frac{\partial \mathcal{H}}{\partial u_1} = W_1 u_1 + \lambda_S \frac{\partial \dot{S}}{\partial u_1} + \lambda_E \frac{\partial \dot{E}}{\partial u_1} + \cdots = 0$$

$$\Rightarrow \quad u_1^* = -\frac{1}{W_1}(\lambda_S \frac{\partial \dot{S}}{\partial u_1} + \lambda_E \frac{\partial \dot{E}}{\partial u_1} + \cdots)$$

$$\frac{\partial \mathcal{H}}{\partial u_2} = 0 \quad \Rightarrow \quad u_2^* = -\frac{1}{W_2}(\lambda_S \frac{\partial \dot{S}}{\partial u_2} + \cdots)$$

$$\frac{\partial \mathcal{H}}{\partial u_3} = 0 \quad \Rightarrow \quad u_3^* = -\frac{1}{W_3}(\lambda_S \frac{\partial \dot{S}}{\partial u_3} + \cdots)$$

$$\frac{\partial \mathcal{H}}{\partial u_4} = 0 \quad \Rightarrow \quad u_4^* = -\frac{1}{W_4}(\lambda_S \frac{\partial \dot{S}}{\partial u_4} + \cdots).$$

Using Pontryagin's Maximum Principle we have the Figures 9 and 10.

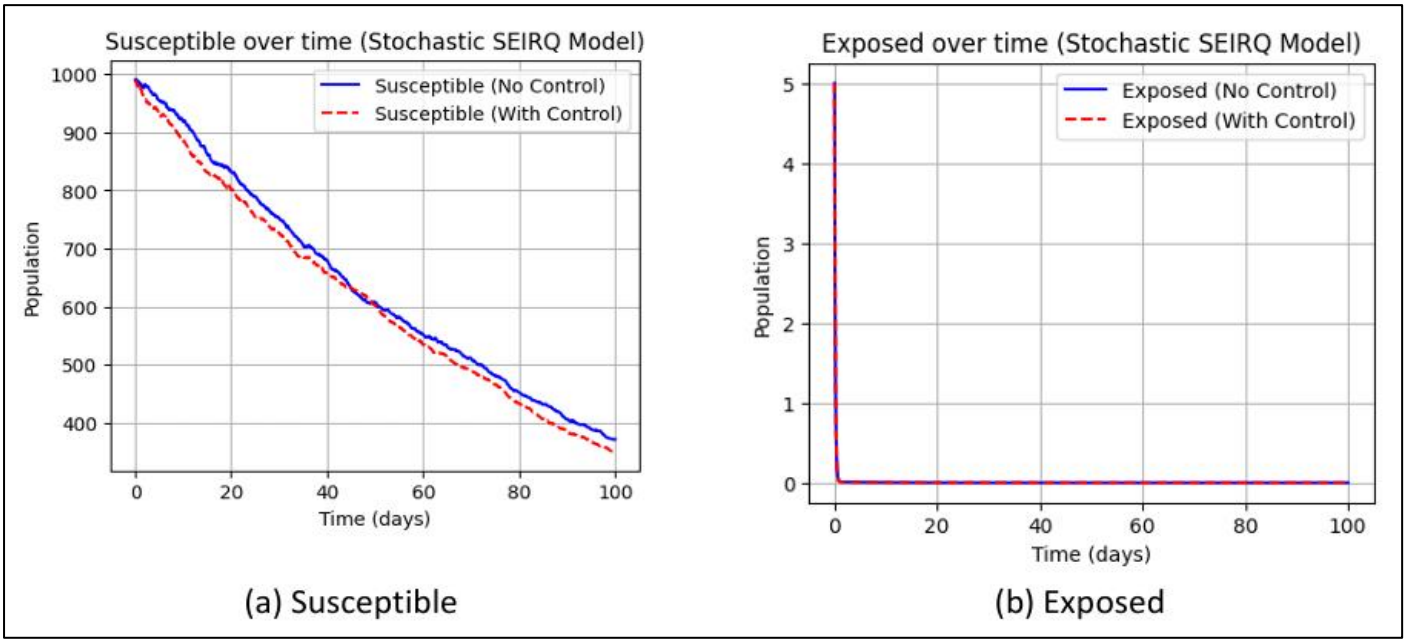

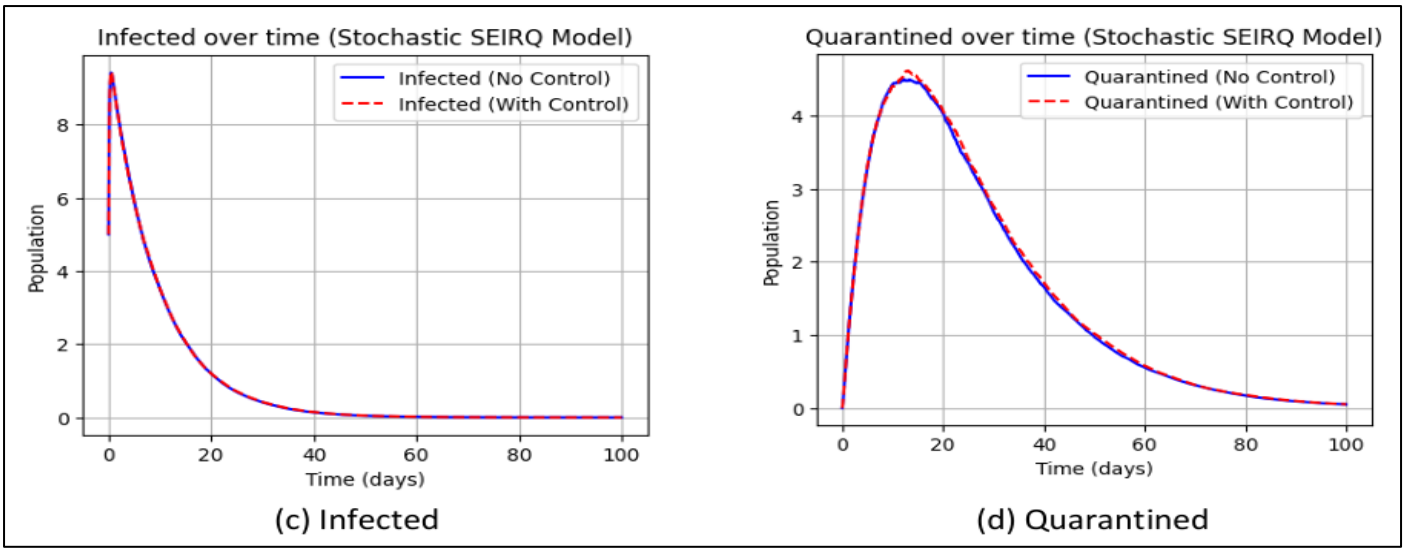

ISSN No:-2456-2165 https://doi.org/10.38124/ijisrt/26jan951

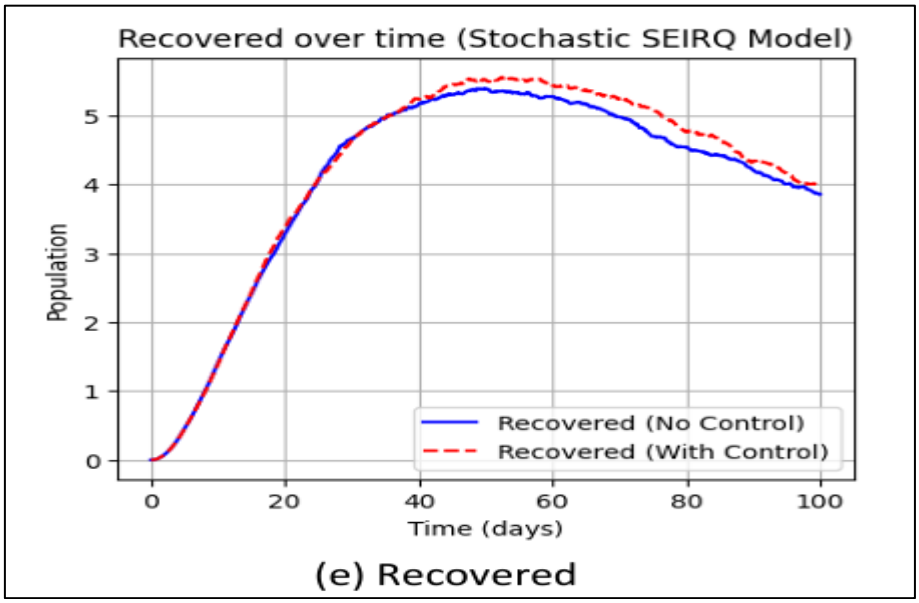

Fig 9 Stochastic Scenario of State Variables with and without Control when $\alpha = 0.05, \theta = 0.2$ and $\phi = 0.1$.

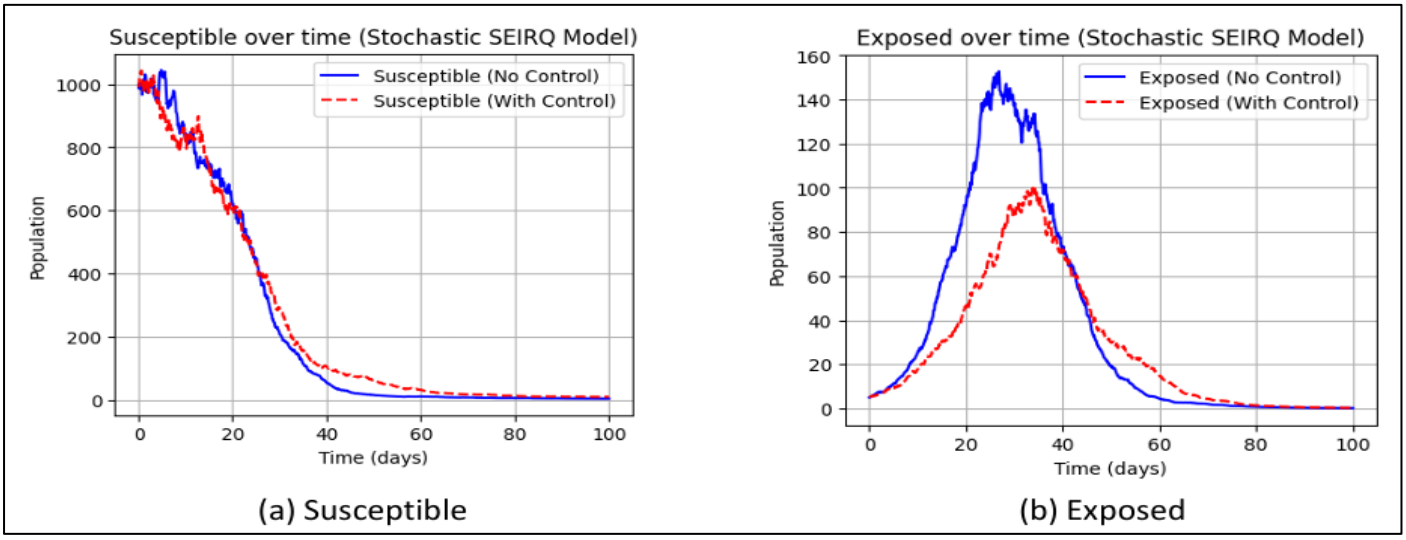

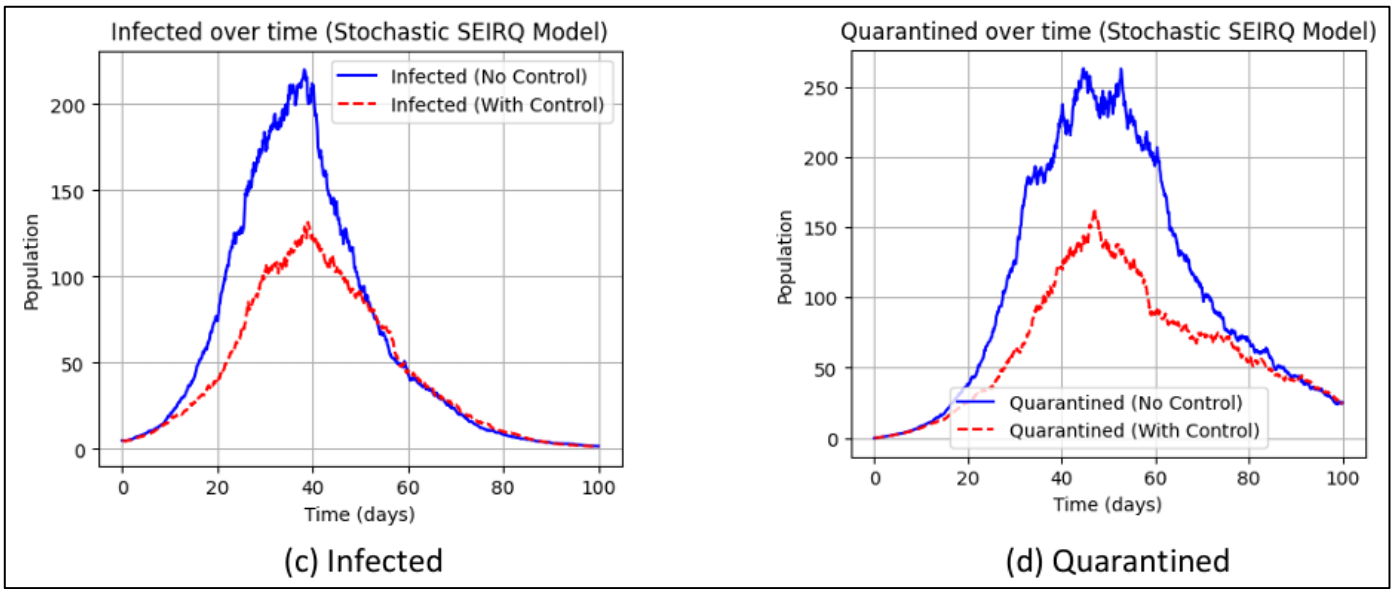

ISSN No:-2456-2165 https://doi.org/10.38124/ijisrt/26jan951

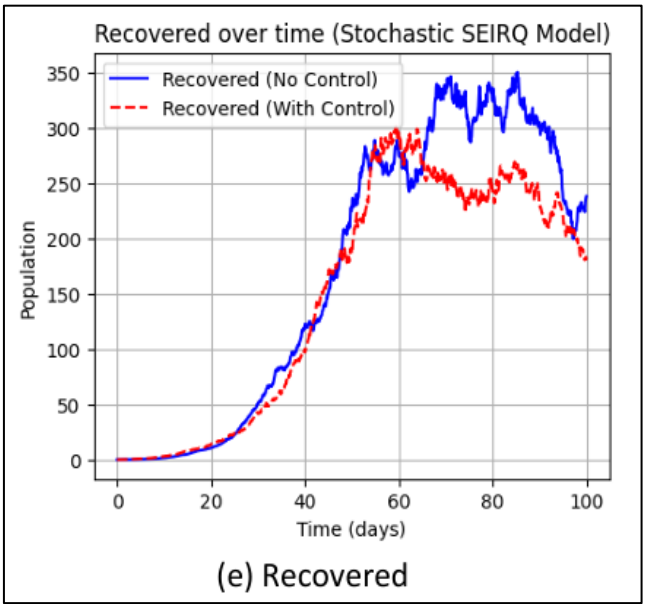

Fig 10 Stochastic Scenario of State Variables with and without Control.

VI. NUMERICAL ANALYSIS

Figure 4 illustrates the temporal dynamics of the susceptible, exposed, infected, quarantined, and recovered populations under scenarios with and without optimal control. In the absence of control measures, the infected population increases rapidly, reaching a higher peak and persisting for a longer duration. When optimal controls are implemented, a significant reduction in the infected and exposed classes is observed, while the susceptible population declines more gradually. The quarantined and recovered populations increase more rapidly under control, indicating effective isolation and treatment. Overall, the results demonstrate that the combined control strategies substantially mitigate disease transmission and accelerate epidemic containment. Figure 5 depicts the impact of varying recruitment rates π on the dynamics of the state variables. As the value of π increases, the susceptible population grows more rapidly, leading to higher exposure and infection levels. Consequently, the infected and quarantined compartments exhibit larger peaks for higher recruitment rates, indicating enhanced transmission potential. The recovered population also increases with larger π values due to the rise in infection cases. These results highlight the sensitivity of influenza transmission dynamics to population recruitment and emphasize the importance of accounting for demographic effects in disease control strategies. Figure 6 presents the effects of different values of the infection rate α on the evolution of the susceptible, exposed, infected, quarantined, and recovered populations. An increase in α leads to a rapid decline in the susceptible class due to higher transmission intensity, while the exposed and infected populations rise sharply and attain larger peak values. The quarantined compartment also expands as more infected individuals are isolated. Conversely, the recovered population increases more rapidly for higher infection rates, reflecting enhanced disease progression. These observations demonstrate that the infection rate α plays a dominant role in shaping epidemic dynamics and significantly influences the severity and timing of influenza outbreaks. Figure 7 illustrates the influence of different total population sizes N on the dynamics of the susceptible, exposed, infected, quarantined, and recovered compartments. As the population size increases, the number of susceptible individuals grows proportionally, creating greater opportunities for disease transmission. This leads to higher peaks in the exposed and infected populations, indicating an elevated epidemic burden in larger populations. The quarantined and recovered classes also increase correspondingly, reflecting intensified isolation and recovery processes. These results suggest that population size plays a crucial role in amplifying influenza transmission and highlight the need for stronger and early intervention measures in densely populated settings. Figure 8 compares the evolution of the infected population under different control scenarios, including no control, single control, dual controls, and the simultaneous application of three controls. In the absence of intervention, the infected class exhibits a rapid increase with a high peak and prolonged persistence. Implementing a single control reduces the infection level moderately, while the combination of two controls leads to a more pronounced decline in both peak magnitude and outbreak duration. The application of all three control measures produces the greatest reduction in infection levels, driving the system rapidly toward disease elimination. This demonstrates the effectiveness of integrated control strategies in suppressing influenza transmission. Figure 9 presents the stochastic evolution of the susceptible, exposed, infected, quarantined, and recovered populations under controlled and uncontrolled scenarios for the parameter values $\alpha = 0.05$, $\theta = 0.2$, and $\phi = 0.1$. These parameter choices correspond to a reduced transmission intensity, a shorter incubation period, and an increased treatment efficacy, respectively. As in Figure 10, the stochastic system is simulated using the Euler–Maruyama method, with solid curves denoting the uncontrolled case and dashed curves representing the controlled dynamics. Compared to the baseline stochastic scenario, a substantial attenuation of disease transmission is observed. The susceptible population remains at a higher level over time, while the exposed and infected compartments exhibit markedly lower peaks and faster decay when control measures are applied. In particular, the infected population is significantly suppressed, indicating the combined effectiveness of reduced transmission and enhanced treatment. Additionally, the quarantined and recovered populations increase more rapidly in the controlled case, reflecting efficient isolation and recovery processes. Overall, Figure 9 demonstrates that appropriate parameter settings, together with optimal control strategies, substantially enhance epidemic containment and reduce stochastic variability in disease dynamics. Figure 10 illustrates the stochastic dynamics of the SEIQR model under the presence and absence of control strategies. Each panel depicts the temporal evolution of one state variable obtained by solving the stochastic system using the Euler–Maruyama scheme. The solid curves correspond to the uncontrolled case, whereas the dashed curves represent the controlled scenario. In the absence of control, the susceptible population decreases rapidly due to sustained disease transmission, leading to a pronounced increase in the exposed and infected

ISSN No:-2456-2165 https://doi.org/10.38124/ijisrt/26jan951

populations. When control measures are implemented, a noticeable mitigation effect is observed: the susceptible class declines more slowly, while both the exposed and infected populations are significantly reduced over time. This reduction is mainly attributed to the combined effects of vaccination, transmission reduction, treatment, and quarantine controls. Furthermore, the controlled system exhibits an increase in the quarantined and recovered populations, indicating enhanced isolation of infectious individuals and improved recovery outcomes. Despite the presence of stochastic perturbations, the controlled trajectories remain consistently lower for the infected class compared to the uncontrolled case, highlighting the robustness and effectiveness of the proposed intervention strategies in suppressing disease spread under random environmental fluctuations.

VII. CONCLUSION

In this work, a comprehensive SEIQR epidemic model incorporating both deterministic and stochastic effects was developed to investigate the transmission dynamics of influenza. The model explicitly integrates vaccination, transmission reduction, treatment, and quarantine as control strategies. Rigorous analytical results, including the derivation of the basic reproduction number and stability analysis of the DFE, were established to characterize the qualitative behavior of the system. An optimal control problem was formulated, and the necessary optimality conditions were obtained using Pontryagin's Maximum Principle, providing insights into effective intervention strategies. To account for environmental and demographic uncertainties, stochastic perturbations driven by independent Wiener processes were introduced, and the system was solved numerically using the Euler–Maruyama scheme. Numerical simulations demonstrate that the combined implementation of control measures significantly reduces infection levels and suppresses stochastic fluctuations. Overall, the results highlight the importance of integrated and timely interventions in controlling influenza outbreaks and provide a robust mathematical framework for epidemic management under uncertainty.

REFERENCES

[1]. [Abdoon and Alzahrani, 2024] Abdoon, M. A. and Alzahrani, A. B. M. (2024). Comparative analysis of influenza modeling using novel fractional operators with real data. *Symmetry*, 16(9):1126.

[2]. [Abdoon et~al., 2023] Abdoon, M. A., Saadeh, R., Berir, M., Guma, F. E., and Ali, M. (2023). Analysis, modeling and simulation of a fractional-order influenza model. *Alexandria Engineering Journal*, 74:231–240.

[3]. [Ahmed et~al., 2023] Ahmed, M., Masud, M. A. B., and Sarker, M. M. A. (2023). Bifurcation analysis and optimal control of discrete sir model for covid-19. *Chaos, Solitons & Fractals*, 174:113899.

[4]. [Alexander et~al., 2004] Alexander, M. E., Bowman, C., Moghadas, S. M., Summers, R., Gumel, A. B., and Sahai, B. M. (2004). A vaccination model for the transmission dynamics of influenza. *SIAM Journal on Applied Dynamical Systems*, 3(4):503–524.

[5]. [Almutairi et~al., 2023] Almutairi, D., Abdoon, M. A., Berir, M., Saadeh, R., and Qazza, A. (2023). A numerical confirmation of a fractional seitr influenza model efficiency. *Applied Mathematics & Information Sciences*, 17(5):741–749.

[6]. [Alsubaie et~al., 2024] Alsubaie, N. E., Guma, F. E., Boulehmi, K., Al-Kuleab, N., and Abdoon, M. A. (2024). Improving influenza epidemiological models under caputo fractional-order calculus. *Symmetry*, 16(7):929.

[7]. [Alzahrani et~al., 2023] Alzahrani, S. M., Saadeh, R., Abdoon, M. A., Qazza, A., Guma, F. E. L., and Berir, M. (2023). Numerical simulation of an influenza epidemic: prediction with fractional seir and the arima model. *Applied Mathematics & Information Sciences*, 18(1):1–12.

[8]. [Andreu-Vilarroig et~al., 2024] Andreu-Vilarroig, C., Villanueva, R. J., and González-Parra, G. (2024). Mathematical modeling for estimating influenza vaccine efficacy: a case study of the valencian community, spain. *Infectious Disease Modelling*, 9(3):744–762.

[9]. [Arun~Kumar and Venkatesh, 2023] Arun Kumar, K. and Venkatesh, A. (2023). Mathematical analysis of SEITR model for influenza dynamics. *Journal of Computational Analysis and Applications*, 31(2):281–293.

[10]. [Ashraf et~al., 2025] Ashraf, M., Muhammad, N., Masud, M. A. B., Alam, M. N., and Hossen, M. J. (2025). Modeling and analysis of dynamic waveforms in nonlinear fractional models of fifth order. *Computational Methods for Differential Equations*.

[11]. [Barik et~al., 2021] Barik, M., Swarup, C., Singh, T., Habbi, S., and Chauhan, S. (2021). Dynamical analysis, optimal control and spatial pattern in an influenza model with adaptive immunity in two stratified populations. *AIMS Mathematics*, 7(4):4898–4935.

[12]. [Imran et~al., 2019] Imran, M., Ben-Romdhane, M., Ansari, A. R., and Temimi, H. (2019). Numerical study of an influenza epidemic dynamical model with diffusion. *Discrete and Continuous Dynamical Systems – Series S*, 13(10):2761–2787.

[13]. [Kanyiri et~al., 2020] Kanyiri, C. W., Luboobi, L., and Kimathi, M. (2020). Application of optimal control to influenza pneumonia coinfection with antiviral resistance. *Computational and Mathematical Methods in Medicine*, 2020:1–15.

[14]. [Kanyiri et~al., 2018] Kanyiri, C. W., Mark, K., and Luboobi, L. (2018). Mathematical analysis of influenza A dynamics in the emergence of drug resistance. *Computational and Mathematical Methods in Medicine*, 2018:1–14.

[15]. [Kharis and Arifudin, 2017] Kharis, M. and Arifudin, R. (2017). Mathematical model of seasonal influenza with treatment in constant population. *Journal of Physics: Conference Series*,

ISSN No:-2456-2165 https://doi.org/10.38124/ijisrt/26jan951

824:012034.

[16]. [Khondaker, 2022] Khondaker, F. (2022). Optimal control analysis of influenza epidemic model. *Applied Mathematics*, 13(10):845–857.

[17]. [Kim et~al., 2016] Kim, S., Lee, J., and Jung, E. (2016). Mathematical model of transmission dynamics and optimal control strategies for 2009 A/H1N1 influenza in the republic of korea. *Journal of Theoretical Biology*, 412:74–85.

[18]. [Lamwong et~al., 2022] Lamwong, J., Pongsumpun, P., Tang, I., and Wongvanich, N. (2022). Vaccinationâ€™s role in combating the omicron variant outbreak in thailand: an optimal control approach. *Mathematics*, 10(20):3899.

[19]. [Lamwong et~al., 2023] Lamwong, J., Wongvanich, N., Tang, I., and Pongsumpun, P. (2023). Optimal control strategy of a mathematical model for the fifth wave of COVID-19 outbreak (omicron) in thailand. *Mathematics*, 12(1):14.

[20]. [Lee et~al., 2010] Lee, S., Chowell, G., and Castillo-Chávez, C. (2010). Optimal control for pandemic influenza: the role of limited antiviral treatment and isolation. *Journal of Theoretical Biology*, 265(2):136–150.

[21]. [Masud and Ahmed, 2018] Masud, A. B. and Ahmed, F. (2018). Comparing theoretical and practical solution of the first order first degree ordinary differential equation of population model. *Open Acc J Math Theor Phy*, 1(1):11–17.

[22]. [Masud et~al., 2021] Masud, M. A. B., Ahmed, M., and Rahman, M. H. (2021). Optimal control for covid-19 pandemic with quarantine and antiviral therapy. *Sensors International*, 2:100131.

[23]. [Masud and Ahmed, 2025] Masud, M. A. B. and Ahmed, M. (2025). Optimal control for system of stochastic differential equations with lévy jumps. *Results in Control and Optimization*, page 100600.

[24]. [Masud et~al., 2017] Masud, M. A. B., Doly, S. A., et al. (2017). A study of stellar model with kramerâ€™s opacity by using runge kutta method with programming c. *International Journal of Astronomy and Astrophysics*, 7(03):185.

[25]. [Masud et~al., 2026] Masud, M. A. B., Rahman, S., Shimi, F. N., Ahmed, M., and Gope, R. C. (2026). Optimizing epidemic control: Nash game approach to stochastic modeling with brownian motion. *Results in Control and Optimization*, page 100657.

[26]. [Masud et~al., 2025] Masud, M. A. B., Tasnim, T., Ahmed, M., and Rahman, M. K. (2025). Dynamic nash game for linear stochastic control with markov jump in mpox. *Results in Control and Optimization*, page 100640.

[27]. [Masud et~al., 2024] Masud, M., Shimi, F. N., and Gope, R. C. (2024). Numerical integration techniques: a comprehensive review. *International Journal of Innovative Science and Research Technology*, pages 2744–2755.

[28]. [Nainggolan, 2022] Nainggolan, J. (2022). Optimal control of influenza A dynamics in the emergence of a two strain. *Journal of Mathematics and Applications*, 16(3):835–844.

[29]. [Nainggolan, 2023] Nainggolan, J. (2023). Optimal countermeasure control on influenza spread model in the emergence of drug resistance. *International Journal of Science and Research*, 12(2):300–306.

[30]. [Ojo et~al., 2022] Ojo, M. M., Benson, T. O., Peter, O. J., and Goufo, E. F. D. (2022). Nonlinear optimal control strategies for a mathematical model of COVID-19 and influenza co-infection. *Physica A: Statistical Mechanics and its Applications*, 607:128173.

[31]. [Parvin et~al., 2025] Parvin, H., Alam, M. N., Masud, M. A. B., and Hossen, M. J. (2025). Investigating traveling wave structures in the van der waals normal form for fluidized granular matter through the modified s-expansion method. *Partial Differential Equations in Applied Mathematics*, page 101285.

[32]. [Pongsumpun et~al., 2023] Pongsumpun, P., Lamwong, J., Tang, I., and Pongsumpun, P. (2023). A modified optimal control for the mathematical model of dengue virus with vaccination. *AIMS Mathematics*, 8(11):27460–27487.

[33]. [Pongsumpun, 2017] Pongsumpun, P. (2017). Mathematical model of influenza with seasons in thailand. In *Proceedings of the Burapha University International Conference*, volume 2017, pages 494–502.

[34]. [Prieto and Ibarguen-Mondragon, 2019] Prieto, K. and Ibarguen-Mondragon, E. (2019). Parameter estimation, sensitivity and control strategies analysis in the spread of influenza in mexico. *Journal of Physics: Conference Series*, 1408(1):012020.

[35]. [Prosper et~al., 2011] Prosper, O., Saucedo, O., Thompson, D., Torres-Garcia, G., Wang, X., and Castillo-Chávez, C. (2011). Modeling control strategies for concurrent epidemics of seasonal and pandemic H1N1 influenza. *Mathematical Biosciences and Engineering*, 8(1):141–170.

[36]. [Qiu and Feng, 2009] Qiu, Z. and Feng, Z. (2009). Transmission dynamics of an influenza model with vaccination and antiviral treatment. *Bulletin of Mathematical Biology*, 72(1):1–33.

[37]. [Rahmalia and Herlambang, 2018] Rahmalia, D. and Herlambang, T. (2018). Weight optimization of optimal control influenza model using artificial bee colony. *International Journal of Computer Science and Applied Mathematics*, 4(1):27.

[38]. [Rahman et~al., 2025] Rahman, S., Prity, F. S., and Masud, M. A. B. (2025). Optimizing indoor visible light communication systems: A comparative analysis of multi-led configurations.

[39]. [Ratti et~al., 2023] Ratti, M., Concina, D., Rinaldi, M., Salinelli, E., Di Brisco, A. M., Ferrante, D., Volpe, A., and Panella, M. (2023). Vaccination strategies against seasonal influenza in long term care settings: lessons from a mathematical modelling study. *Vaccines*, 11(1):32.

[40]. [Sabir et~al., 2022] Sabir, Z., Said, S. B., and Al-Mdallal, Q. (2022). A fractional order numerical study for the influenza disease mathematical model.

ISSN No:-2456-2165 https://doi.org/10.38124/ijisrt/26jan951

Alexandria Engineering Journal, 65:615–626.

[41]. [Varshney and Dwivedi, 2021] Varshney, K. G. and Dwivedi, Y. K. (2021). Mathematical modelling of influenza–meningitis under the quarantine effect of influenza. *Turkish Journal of Computer and Mathematics Education*, 12(11):7214–7225.

[42]. [Waleed et~al., 2015] Waleed, M., Imran, M., and Khan, A. (2015). Stochastic analysis of an influenza epidemic model. *International Journal of Applied and Computational Mathematics*, 3(2):425–443.

[43]. [World Health Organization, 2018] World Health Organization (2018). Influenza: Data and statistics. Accessed: 2018.